Integrated Solar Panel Antenna Array for CubeSats (ISAAC)

Taha Yekan, Muhammadeziz Tuyghur, Serhat Altunc, Eleanya E. Onuma, and Marta B. Shelton, and Reyhan Baktur *Senior Member, IEEE*

***Abstract*—This paper presents an integrated solar panel antenna array for CubeSats (ISAAC), which is an optically transparent reflectarray printed on the cover glass of a solar panel. The optical transparency of the antenna is 95% and with the 92% transparent cover glass, ISAAC has been measured to only reduce the efficiency of a triple junction solar cell from 29% (bare cell) to 24%. The antenna operates at 8.475 GHz, has a measured gain of higher than 21 dB after a full integration with the solar panel and after being conformal coated with Parylene HT for withstanding harsh elements. ISAAC is inkjet printed using conductive ink on a piece of 20 cm $\times$ 30 cm space certified glass. All components, from the antenna to solar panel, are commercial-off-the-shelf (COTS), space certified, and suitable a space deployment. Detailed analysis of different low-profile unit cells, loss due to conductive ink, effect of solar cells, and loss due to assembly are discussed, and methods to improve the antennas performance under these loss factors are presented.**

***Index Terms*—CubeSat, inkjet printing, reflectarray, solar cell, integration, Transparent antenna**

I. INTRODUCTION

THE rise of CubeSats has pushed antenna designs suitable for these platforms to the forefront [1]. High-gain antenna arrays, in particular, are of interest for downlinking high data rates from low Earth orbit (LEO) [2] or for use as relays from deep space [3]. In both cases, reflectarray antennas were integrated on a surface that is not occupied by solar cells. The majority of CubeSats' surface, including the bottom of specific missions such as SPORTS [4], is covered with solar cells. This is to ensure that the satellite has enough power, including when it is tumbling after being launched. It is therefore desirable not to remove any solar cell in order to fit in a traditional patch or array antenna. This motivates the goal of integrating high gain optically transparent antenna array with the solar cells and maintain the proper functionality of both antenna and solar cells. Such an integrated solar panel antenna array for CubeSats (ISAAC) can be instrumental when the communication front and the sun are on the same direction, such as transmitting from LEO to upper orbits, from Lunar orbit to Earth, and for any Lunar and Mars missions including but not limited to rovers and orbiters.

Low profile (such as cross dipole) or transparent antenna arrays integrated with solar cells have been presented [5]–[9]. Moharram et al.'s design is to create holes in the stacked acrylic layers to achieve required phase shift [9]. As the acrylic cover glass is relatively thick, even with the holes, it blocks about 15% of the light. The reflectarrays presented in [6], [7] were printed directly on solar cells, but those solar cells may require custom fabrication. In addition, as is seen in this paper, the square loop unit cells present better reflectarray performance compared to the cross dipoles reported by [5]–[7]. The design by Dreyer et al. serves as a helpful reference, although the solar cells are not for space use [8]. Antenna design and integration methods for different solar cells other than the ones for space use have also been presented [10]–[13], with interesting applications from aircraft to remote sensing, Internet of Space Things, and wide band applications.

This paper presents a reflectarray of transparency higher than 95% inkjet printed on space certified cover glass at X band on a relatively small panel (i.e. 200 mm $\times$ 300 mm to fit on a 6U CubeSat) with improved aperture efficiency compared to the reported designs. The CubeSat terminology such as 6U can be found in documents [14], [15]. ISAAC design does not require custom-made solar cells or complex integration. All components are commercial-off-the-shelf (COTS), space certified, and suitable for tests such as thermal vacuum bake-out and vibration for a space deployment. The paper builds on previous studies [16]–[19] and extends them with complete design data, detailed analysis on loss factors due to prototyping and integration, fully integrated prototype, and assessments of both antenna's and solar panel's performance.

A. ISAAC Geometry and Design Objectives

ISAAC is a reflectarray and consists of a ground plane, substrate (i.e. cover glass and solar cells), and antenna elements printed on the glass. It has elements with different sizes, and is fed by an antenna that can be a horn or a planar array antenna (Fig. 1). The geometrical shape and dimension of the array elements are carefully determined to supply sufficient required phase to compensate the phase of the incoming wave from the feed, and to provide the dedicated phase to produce the desired reflected beam angle. This is explained by (1), where it calculates the required reflection phase ϕ_r by the i^{th} element on the xy plane (Fig. 1) to point the reflectarray's beam to (ϕ_0, θ_0). In (1), k_0 is the free-space propagation constant, (x_i,

This paragraph of the first footnote will contain the date on which you submitted your paper for review. The majority of this work was supported by the SmallSat Technology Partnerships (STP) element of NASA's Small Spacecraft Technology Program (SSTP). The printer for prototyping was purchased with a Defense University Research Instrumentation Program (DURIP) award sponsored by the Office of Naval Researc

Taha Yekan, MuhammadEziz TursunNiyaz, and Reyhan Baktur are with the Department of Electrical and Computer Engineering, Utah State University, Logan, UT 84322 USA (e-mail: reyhan.baktur@usu.edu).

Serhat Altunc, Eleanya E. Onuma, and Marta B. Shelton are with NASA Goddard Space Flight Center, Greenbelt, MD 20771.

y_i) is the position of array element, d_i is the distance from the phase center of the feed (e.g. the horn) to the center of the i_{th} element, and N is an integer [20].

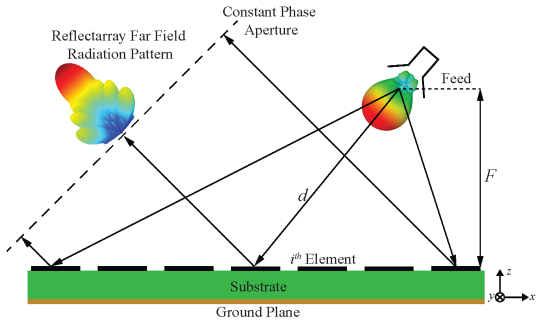


Fig. 1: Illustration of a Reflectarray.

$$\phi_r = k_0[d_i - (x_i \cos\phi_0 + y_i \sin\phi_0)\sin\theta_0] \pm 2N\pi. \quad (1)$$

Design objectives of ISAAC is summarized in Table I. It produces a reflected beam normal (z axis) to the face of the reflectarray (xy plane) while the feed is at 22.7° from the normal direction. This avoids blockage of the reflected field by the feed and facilitates integration of the feed on one face of a CubeSat, with ISAAC is on the deployed panel, as in [2], [3]. The 22.7° angle can be readily adjusted to suit specific CubeSats. ISAAC has a linear polarization, but supports both TE and TM incidence and can be modified to achieve circular polarization to eliminate any link degradation due to polarization mismatch [21]. The frequency is chosen so that ISAAC can be supported by Near Earth Network (NEN), Direct-to-Earth (DTE), and Deep Space Network (DSN) of NASA.

TABLE I: ISAAC Design Objectives

Size	20 cm × 30 cm
Frequency	8.475 GHz
Polarization	Linear
Beam direction	Normal to ISAAC
Feed direction	22.7° from the normal direction
Gain	> 20 dB
Transparency	≈ 95%

B. Choice of Material

Although there were reported designs where the reflectarray elements were directly printed on individual pieces of solar cell with the cover glass of solar cells acting as the dielectric substrates, the thickness of those glass is not sufficient for an X band operation. Therefore a thicker glass is needed. Or, it is possible to lift a large piece of glass off from solar cells and use the glass together with the air or vacuum in between the glass and solar cells as the substrate. In this configuration, the glass does not have to be as thick. But using only one piece of glass, even though relatively thick, simplifies the design process and there is an interest in using thicker cover glass for missions in deep space for additional protection against radiation, micrometeorite impacts, and extreme environmental conditions [22]. Therefore, we have chosen to use a single piece of commercial AF32 glass [23] that has high transmittance (92%) and high temperature tolerance desirable for space applications as the substrate. The AF32 glass has been measured to have a dielectric constant (ϵ_r) of 4.5 and loss tangent ($\tan\delta$) of 0.015 at X band [8].

The height of the AF32 substrate is critical in affecting the performance of the reflectarray, where the thickness needs to be sufficient to support necessary phase range. When the glass is too thin, the radiation Q is greater than element Q (under coupled) [24]. For the AF32 glass, it is found that the thickness of 1.5 mm is the critically coupled condition that happens when radiation Q is equal to element Q as described by the study [24]. Therefore the thickness of the cover glass needs to be bigger than 1.5 mm to operate at the over coupled condition to yield an applicable phase response. Considering fabrication feasibility, a trade-off has to be made between the phase range and slope of the phase response. As described in Section II, the thickness of the AF32 is chosen to be 2.5 mm after examining the element geometry and phase response.

As the thickness of the cover glass is much larger than that of most solar cells for space applications, the effect of the solar cells on the reflectarray's gain due to the phase error is not substantial. But the gain reduction due to solar cells being lossy at X band has to be evaluated as presented in Section III-A. This places less restriction on the choice of solar cells. Because the purpose of this design is to provide a near mission-ready solar panel antenna solution, we have chosen space certified SolAero ZTJM solar cells (29% efficiency, now ZTJ series by Rocket Lab) [25].

C. Factors for Gain Reduction

The reflectarray is printed on a single piece of cover glass and then integrated on top of a solar panel. The gain of the reflectarray, or the aperture efficiency is affected by the printing, assembly such as air gaps and use of adhesives, and the solar cell which serves as a thin lossy substrate. The reflectarray elements can be either screen printed or inkjet printed on the glass using conductive ink or paste. With either method, the conductivity of the ink or paste is not as high as a solid conductor such as copper. In addition, the thickness of the printed trace is often less than 5 μm for inkjet printing. The limited conductivity and thickness of the material result in Ohmic loss and therefore the gain reduction of the reflectarray. Screen printing may yield thicker traces but may sacrifice the precision. Other deposition methods such as aerosol jet printing and cleanroom-based process also face challenges in thickness of the trace in addition to the cost.

Assembling the glass (with reflectarray printed on it) on solar panel will inevitably created an added layer such as air gap, or the adhesives used to bond the glass to the solar panel. Also, in order not to press the solar cells, and to create a channel for the possible heat from electrodes to dissipate, it is desirable to leave some space between the glass and the solar panel. These layers and gap will be considered in the reflectarray design as best as possible, but there is always some

error due to assembly tolerance or communication between the design and assembly crew. The added layer affects the unit cell's response and results in phase error, which leads to the gain reduction.

A solar cell is a lossy layer between the glass and the ground plane. The effect of solar cells on individual patch antenna has been studied [26]–[28]. The reflectarray in this paper takes advantage of sub-wavelength unit cells, which improves the gain and aperture efficiency at the presence of lossy substrate.

The three main factors of gain reduction are studied and quantified in this paper.

II. Reflectarray Design

Fig. 2 is an illustration of the proposed reflectarray (Fig. 2a) and assembly information (Fig. 2b), where the reflectarray elements are printed on a piece of AF32 glass. The solar cells are sandwiched between AF32 and a copper (or aluminum) ground plane. The assembly is a low–cost modular design as the printed glass can be fitted onto an existing solar panel larger than 20 cm $\times$ 30 cm without requiring a custom design. Three candidates for the unit cells (Fig. 2c)— a cross dipole, a square loop, and a meshed patch— were examined in terms of reflection magnitude and phase for the lattice size of $\lambda/2$ and $\lambda/4$, where λ is the free-space wavelength at 8.475 GHz. All three candidates are of low profile that will only block minimal percentage of light, and symmetric to enable both linear and circular polarizations. Although the meshed patch geometry has been extensively examined as a single antenna solution for solar cell integration and has an impending flight opportunity [29], [30], it is found that their advantage as a unit cell for a reflectarray is not significant. In addition, the geometry produces less optical transparency compared to the loop or cross dipole, and requires longer printing time. Therefore, the mesh geometry is not further examined beyond the initial study [17].

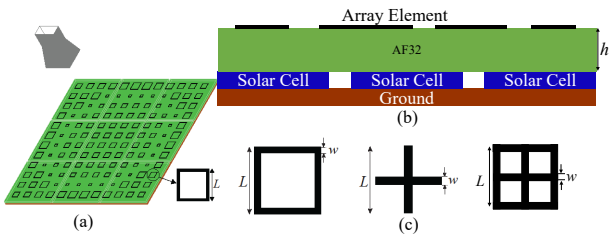


Fig. 2: Illustration of ISAAC Assembly.

A. Examination of the Unit Cells

Geometry of the two types of reflectarray elements is as presented in Fig. 2c and they are printed on the AF32 cover glass backed by the ground plane. Each unit cells were studied using Ansys' HFSS by adapting periodic boundary conditions and Floquets excitation with normal incident fields to extract element phase response for different lattice sizes at 8.475 GHz. The unit cells were first simulated without the solar cells and then with them by inserting the solar cell model [28] in between the glass the ground plane.

When examining the cross dipole and loop unit cells, the width W (Fig. 2c) was chosen to be 0.25 mm by balancing the minimal coverage (i.e. sufficient optical transparency) and a feasible fabrication. The length L was kept to be the variable to tune the reflection for a given substrate height h. Figs. 3 and 4 are reflection phase and magnitude of the two unit cells with the $\lambda/2$ lattice size for a varied h under the normal incident. These figures apply to both TE and TM incidence due to symmetry. It is seen that h needs to be at least 1.5 mm in order to provide an acceptable phase range, corresponding to the critically coupled case [24]. But the phase curve is too sharp at this h value. Increasing h shows reduction of phase range but smoother phase variations. Considering all these, $h = 2.5$ mm was chosen as a reasonable substrate thickness that provides good trade–off between phase range and feasible phase curve for fabrication.

It is also seen that both cross dipole and loop geometry can be potential candidates for a reflectarray with elements spaced at $\lambda/2$, while the loop geometry has reduced cell size. This is consistent with former studies as the loop presents an intrinsic inductance which contributes to a resonance at a smaller geometry compared to dipoles [31].

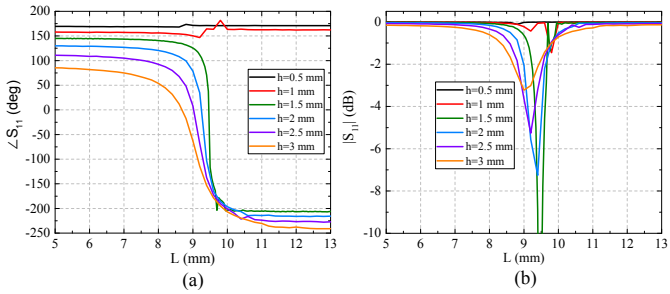


Fig. 3: Cross Dipole of $\lambda/2$ Lattice Size.

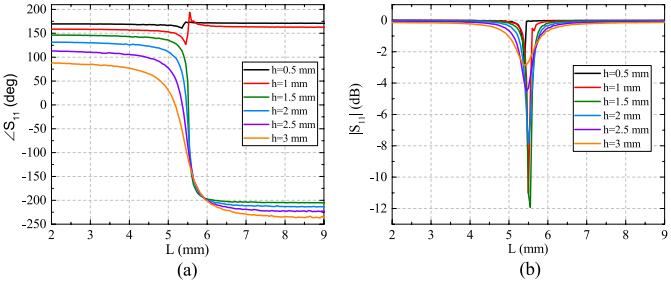


Fig. 4: Loop of $\lambda/2$ Lattice Size.

Reducing cell periodicity to sub-wavelength has been shown to provide special features such as broadening the gain bandwidth and being effective to design reflectarray on lossy substrates [32], [33]. As solar cells are knows to be lossy [26]–[28], a sub-wavelength design is naturally appealing. Both cross dipole and loop unit cells were examined for different sub-wavelength lattice sizes and the results are summarized in Figs. 5, 6. These figures confirm that working at the sub-wavelength shrinks the phase range and reduces the reflection loss at the same time, as shown in [32]. It is seen that both elements are suitable for an array design when the lattice

size is $\lambda/2$ or $\lambda/3$. When the lattice size is reduced to $\lambda/4$, however, the phase range of the cross dipole is limited (less than 270°) and cannot provide sufficient coverage required for a reflectarray design. Loop unit cell, on the other hand, still works well for a $\lambda/4$ lattice. The circle with arrow on Figs. 5, 6 marks the range of L that supports a minimum 270° phase range. It is also observed that the return loss levels for both elements are approximately the same for the same lattice size.

Based on these results, the loop element with $\lambda/4$ lattice spacing was chosen for the ISAAC implementation.

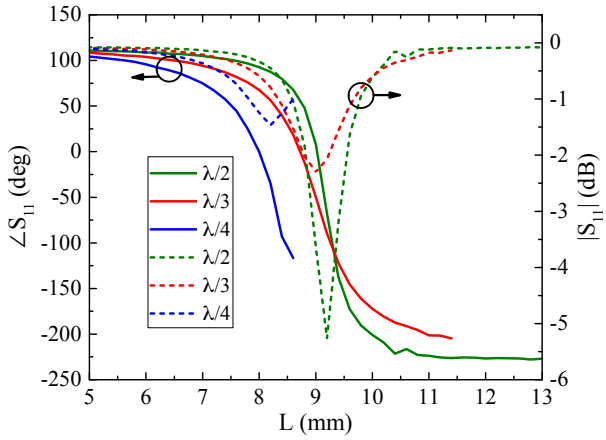


Fig. 5: Cross Dipole Sub-wavelength Lattice Size.

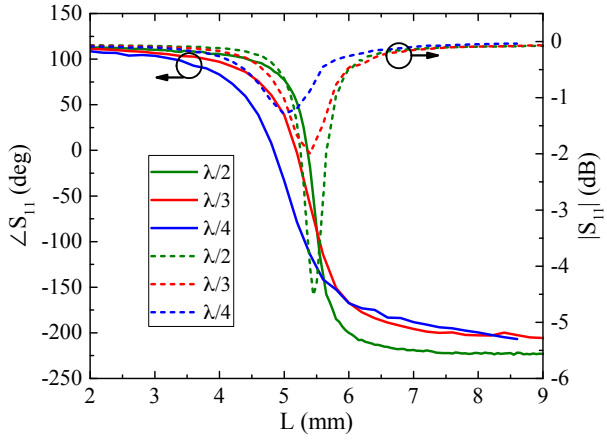
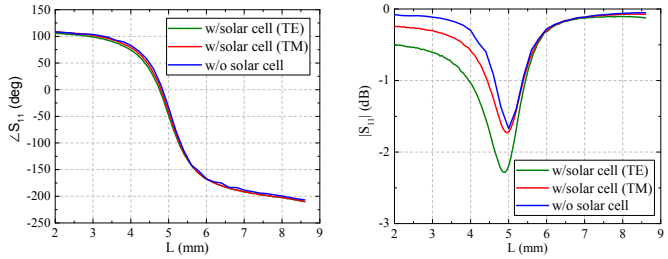


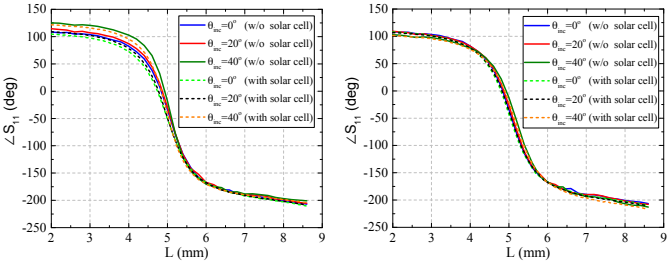
Fig. 6: Loop Sub-wavelength Lattice Size.

To assess the effect of lossy solar cells, including the electrodes (i.e. silver wires parallel to the width of solar cells), on the reflectarray design, material and layer information of a common space solar cell as extracted in [28] and the electrodes were inserted between the glass and the ground plane of a $\lambda/4$ square loop unit cell, and then studied with full-wave simulation. The unit cell performance at at both normal and oblique incidence were studied and the results are summarized in Figs. 7, 8. Fig. 7 also includes the TE and TM plane wave incidence, where the E field of TM wave being parallel to the electrodes and TE being perpendicular. It is seen that the solar cell has little effect on the phase response, but it introduces loss (Fig. 7.b), which is expected. The phase response for the oblique incidences further indicates that there is no significant effect from the solar cell. These results were observed mainly because the thickness of the solar cell is insignificant compared to the cover glass at the design frequency. When the frequency is increased to Ka band or higher, the thickness of the cover glass becomes around or less than 0.5 mm. In that case, the thickness of the solar cell may affect the phase curve and should be carefully examined before generating the full reflectarray. The loss due to the solar cells is further studied in Section III.



(a) Phase Response. (b) Magnitude.

Fig. 7: Loop Element Response at Normal Incidence.



(a) TE (b) TM

Fig. 8: Loop Element Phase Curve at Oblique Incidence.

B. Reflectarray Design Results

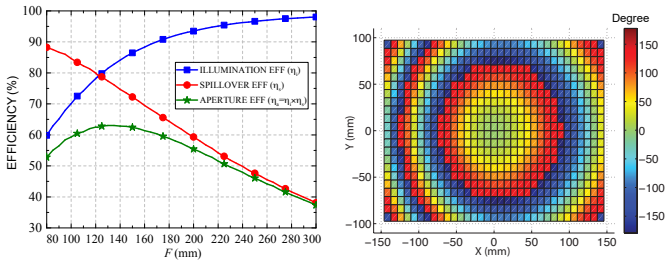
The size, main beam, and feed beam of the reflectarray are as listed in Table I. The focal distance F (Fig. 1) is determined to yield the maximum aperture efficiency, which is the product of illumination and spillover efficiency [34]. Considering an edge taper of -10 dB as a reasonable feed design [20], the illumination, spillover, and aperture efficiency for a 20 cm × 30 cm panel is plotted as function of F in Fig. 9a. It is clear that a focal distance of 135 mm is optimal, and accordingly the gain of the feed is calculated to be 12 dB.

Once F is fixed, the required reflection phase at each element was calculated from (1) and then the length of the unit cell is extracted from the phase curve (Figs. 7, 8). The reflectarray geometry can then be created by using Matlab to script HFSS or directly scripting with the Iron Python embedded in HFSS. Both methods have been adopted and there was not a visible difference in the speed. With Iron Python, however, there is no need of using another program (Matlab) besides HFSS and it has a shorter learning curve, which is appealing for education purpose. In addition, with the Iron Python scripting, all the layers and boundary conditions

can be completed at the same time when the geometry is created.

The completed reflectarray geometry was then studied with full wave simulation by importing a 3D model of a 12 dB horn. At this time, however, the solar cell was not included because such a thin geometry, together with electrodes makes the simulation very slow and affects the accuracy. The effect of solar cells can be estimated analytically and further extracted more accurately/realistically from measurements as presented in the following sections.

The resulting phase distribution is shown in Fig. 9b with L been truncated to the accuracy of 0.01 mm for the ease of fabrication. As seen, the phase distribution exhibits a continuous and symmetric variation across the aperture, with only discontinuities arising from phase wrapping at $\pm 180°$. Therefore, it is concluded that the reflectarray design promises reasonable phase compensation to form the beam at the desired direction.



(a) Aperture Efficiency (b) Phase Map

Fig. 9: Aperture Efficiency and Phase Map.

Simulated radiation patterns are plotted in Fig. 10, and the gain as well as aperture efficiency are listed in Table II. As seen, side lobe and cross polarization levels are well below 20 dB and the gain is sufficient that even if the loss due to solar cells and conductive ink is 4 dB, the design objective in Table I will be met. It should be noted that the gain reduction due to solar cells have been measured to be below 3 dB for antennas integrated on top at different frequencies [26], [27] . It is seen in Section III that the reduction is lower for sub-wavelength designs with thicker substrate.

C. Optical Transparency

The optical transparency due to the reflectarray is computed from (2), where A_{metal} and A_{panel} are the area covered by the printed metal and the area of the solar panel,

$$T_{\text{ant}} = (1 - \frac{A_{\text{metal}}}{A_{\text{panel}}}) \times 100. \qquad (2)$$

In the case of the presented loop antenna elements, the area covered by the metal is

$$A_{\text{metal}} = \sum_i 4(L_i - w)w, \qquad (3)$$

which can be evaluated with a simple code or, more conveniently by using the "Measure Face" function in HFSS' Modeler. The overall transparency is determined by multiplying

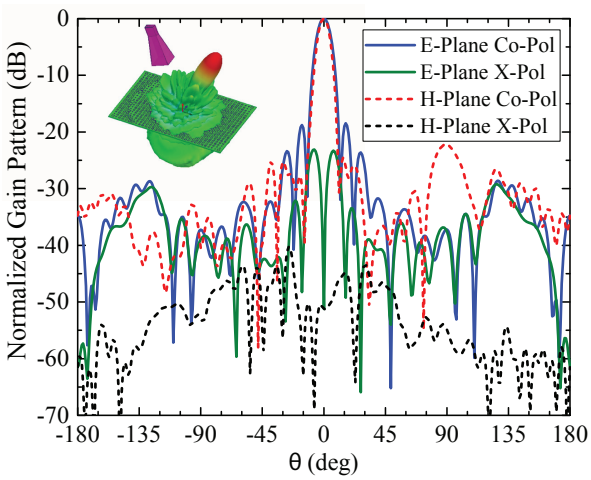


Fig. 10: Simulated Reflectarray Radiation Patterns.

the transparency of the AF32 cover glass and T_{ant}, which is calculated and included in Table II.

TABLE II: Full-wave Simulated Performance

Orientation	Gain (dB)	η_{ap} (%)	T_{ant} (%)
TE	24.37	45.5	94.54
TM	24.78	50	94.54

III. ANALYSIS ON LOSS AND IMPROVEMENT VIA SUB-WAVELENGTH DESIGN

The main factors contributing to the reflectarray's gain reduction were outlined in Section I-C. A detailed analysis of each factor is as follows. Dielectric loss due to the substrate is already included in the loss tangent and therefore not examined.

A. Effect of Solar Cells

Multi-junction space solar cells are made of very thin layers of doped semiconductor and cause a gain reduction for antennas integrated on top of them [28]. It has been shown that using a thicker substrate and adopting sub-wavelength spacing mitigates gain reduction when a reflectarray is fabricated on a lossy substrate [32]. To assess the effect of solar cells, the $\lambda/4$ sub-wavelength reflectarray's radiation efficiency is calculated from (4) based on the unit cell response [31], where Γ_i and T_i are reflection and illumination magnitude of the i^{th} element. We validated the formula by computing η_r, which is -0.64 dB from (4) for the reflectarray without solar cells and compared it with the full wave simulation result of -0.51 dB. As the agreement is very good, we used the formula and the unit cell response at the presence of solar cell (Fig. 7), where $|\Gamma_i|$ can be extracted, to compute the array's gain and aperture efficiency (η_{ap}). By doing so, a full wave simulation for the entire array with solar panel model is avoided. The method may not present the most accurate assessment on the gain reduction due to solar cells because (1) commercial solar cells can be different from vendor to vendor, (2) the solar cell model

extracted in [28] does not include doping and therefore the permittivity and conductivity of each layer may not represent the reality, and (3) the electrodes included in our model is of estimated numbers and dimensions. But this method gives a relative estimation and is useful in keeping the overall design goal at check. For example, the estimated loss due to the solar cells, computed from η_r is lower than 1 dB, which is an indication that the sub-wavelength design on a 2.5 mm glass substrate promises a lower gain reduction compared to what we have seen before [26], [27]. With the simulation results in Table II, the design is deemed suitable for prototyping and final measurements.

$$\eta_r = \frac{\sum_i (|\Gamma_i|^2 \, |I_i|^2)}{\sum_i (|I_i|^2)}. \tag{4}$$

B. CONDUCTOR LOSS

The reflectarray elements were fabricated using inkjet printing with conductive ink, resulting in traces of limited height and conductivity. The trace height can be increased by printing multiple layers on the same trace, but only up to a point where further printing causes the ink to spread, which would reduce the printing precision. Fig. 11 is a scanning electron microscopy (SEM) image of a printed trace. The trace was created by printing three times. It is seen that the height of the trace is around 3 μm. The printed geometry is often cured in an oven to improve the conductivity. But the highest achievable conductivity of the type of ink used by the printer is 3.6×10^6 [35], which means the height of the printed trace is comparable to one microwave skin-depth of the cured conductive ink at the operation frequency. Therefore, there is considerable Ohmic loss on the printed conductor and will result in the antenna's gain reduction.

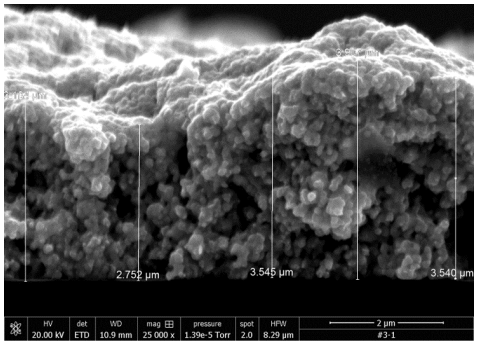


Fig. 11: SEM Image of an Inkjet Printed Line.

The gain reduction caused by the inkjet printing can be substantial for patch (solid or meshed) antennas on substrates of typical thicknesses, such as 1.5 mm for X band or 2 mm for S band. For example, the antenna in [30] has been measured to have more than 4 dB gain reduction when inkjet printed, which necessitated a change in the fabrication method. But since ISAAC is printed on a relatively thick glass and uses sub-wavelength spacing, the gain reduction due to the conductor loss is estimated to be less severe. This is supported by the study shown in Fig. 12, where the square loop unit cell was examined for different lattice spacing, conductivity, and AF32 glass thickness (2.5 mm, and 2 mm for the thinner substrate). The lossy conductor in the study has a height of 3 μm and a conductivity of 3.6×10^6 to represent the inkjet printed traces. The performance of such a printed element is compared with the one made of perfect electric conductor (PEC). Results in Fig. 12 are as expected, where the reflection loss is reduced for the sub-wavelength lattice spacing and thicker substrates. The loss observed for the PEC element is due to the loss tangent of AF32.

An additional study on the conductor loss was performed by using a substrate with all properties the same as the 2.5 mm thick AF32, except for a zero loss tangent. For a faster simulation, instead of entering the conductivity and height for the conductor, a surface resistance of 0.1 Ω□, corresponding a conductivity of 3.3×10^6 S/m and height of 3 μm, was used[1]. The result of this study is presented in Fig. 13. As expected, when the surface resistance of the elements of a $\lambda/2$ unit cell is reduced to half (0.05 Ω□), the reflection magnitude reduces. However, it is still outperformed by a $\lambda/4$ unit cell with 0.1 Ω□ surface resistance. This indicates that the conductor loss in a sub-wavelength reflectarry is reducded not just due to the decrease in the element size (i.e. Ohmic loss area) but also because of the coupling between the elements giving rise to higher effective length for increased reflection.

The loss reduction due to inkjet printing can be estimated from (4) as well, and the value is smaller than 0.5 dB. The actual loss reduction may vary because the height of the printed traces may not be uniform. But the study on the conductor loss confirms that inkjet printing is an effective and reasonable method to prototype ISAAC.

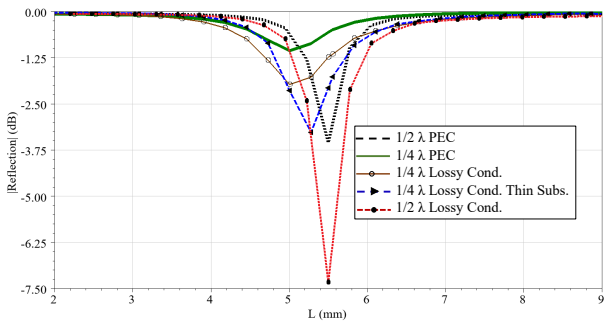


Fig. 12: Effect of Sub-Wavelength Design on Conductor Loss.

C. Loss Due to Gaps in Assembly

After printing the reflectarray on the glass, it is then assembled onto a solar panel (Fig. 14). The cover glass is either attached to the solar panel with transparent adhesive or lifted off with a spacer so that the glass does not press

[1]It should be noted that Ω□ is a unit on its own. As the unit of surface resistance is the same as resistance, a square sign is added to differentiate it. Another widely used notation for the unit of surface resistance is Ω/□, which is the resistance between the two opposite sides of a square made of the material of interest. The surface resistance is independent of the size of the square.

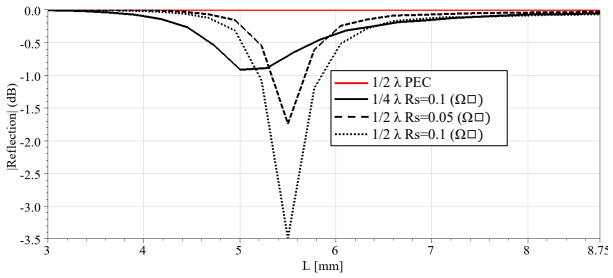
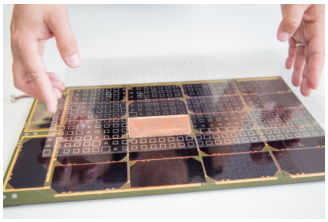
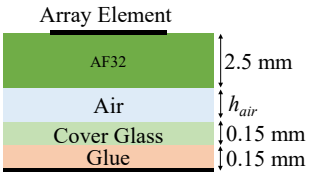


Fig. 13: Reflection Magnetude of Different Unit Cells.

the solar cells and the electric connections. In addition, most commercial solar cells purchased for in-house assembled solar panels have their own cover glass, even if the cells are labeled as "bare cell". In ISAAC design, both the solar cell's own cover glass and the glue layer were included in the unit cell simulation, but not the air gap. The added air gap (or adhesive) during the assembly, if more than 1mm , will result in phase error and accordingly a gain reduction. The effect were studied with full wave simulation and summarized in Table III.



(a) ISAAC Assembly.



(b) ISAAC Layers.

Fig. 14: ISAAC Assembly.

TABLE III: Effect of h_{air} on the Phase Range and Gain

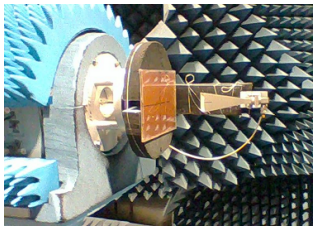
h_{air} (mm)	0.1	0.4	0.8	1.2	> 2.0
Phase Range (deg)	309.9	294.3	279	253.6	< 200
Gain (dB)	24.4	24	23.4	22.4	< 18

IV. FABRICATION AND MEASUREMENTS

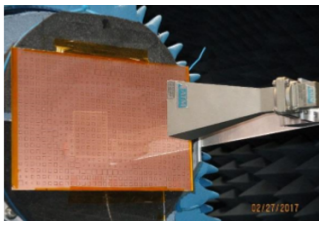
The final design of ISAAC was inkjet printed on a 2.5 mm AF32 glass using Dimatix Materials Printer [36] at Utah State University (USU). The fabricated reflectarray was then measured at USU using a planner near-field scanner in an anechoic chamber. A horn antenna with a 12 dB gain was fabricated using 3D printing and spray painted with conductive ink (the horn is seen in Fig. 22). The antenna was then shipped to NASA Wallops Flight Facility (WFF) for further measurements, integration with solar panel, and evaluation of the solar panel under the reflectarray.

The measurement set-up at WFF is shown in Fig. 15, where a fixture was custom-made to hold the horn feed at the focal distance and to create a 22.7° incidence at the center of the array (Fig. 16). The horn used at WFF is of 15 dB gain and therefore it produces a slightly improved spillover efficiency but reduced illumination efficiency. But the overall aperture efficiency is comparable to the 12 dB horn.

After the initial measurements at USU and WFF, it was decided that the printed array needed to be treated to withstand normal handling without the traces getting scratched off. The next sets of printed glass were then coated with Parylene HT, a specialized, high-performance conformal coating engineered for extreme environments, to improve performance. It is optimized for high-temperature stability (up to 450 C°), long-term UV resistance, low dielectric constants, and superior penetrating capability for conformal coating for space applications. It was applied to a thickness of 0.5 mil to 1 mil at WFF.



(a) Glass Array Under Test.



(b) Glass Array Close-up.

Fig. 15: Measurement Set-up for the Inkjet Printed Reflectarray on Glass.

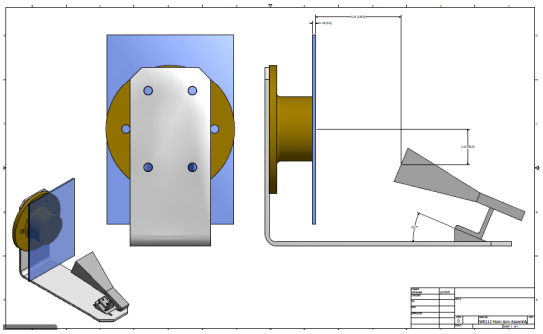
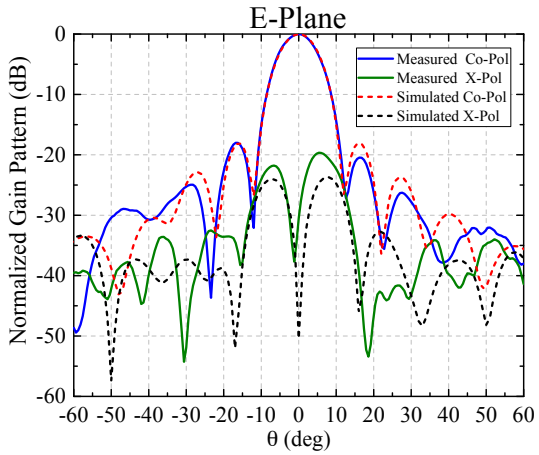


Fig. 16: Mechanical Drawing of the Test Fixture.

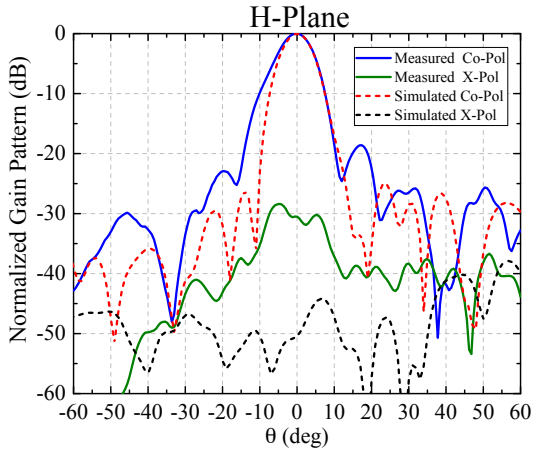
A. REFLECTARRAY PERFORMANCE

Fig. 17 is the radiation patterns of the inkjet printed reflectarray on AF32 glass measured at USU. The solar panel is not included in this test. The reflectarray is then placed on a 6U solar panel (Fig. 14a) borrowed from the Space Dynamics Laboratory (https://www.sdl.usu.edu), and backed by a ground plane. The measured radiation patterns are plotted in Fig. 18.

It is seen that the main beam is normal to the reflectarray (this angle is indexed as 0° for the near-field scanner) as designed, and the measurements agrees well with the simulation. The side lobe level as well as cross polarization level are also in acceptable range. It is also observed that the beam is widened slightly when the solar panel is placed under, indicating a reduction in the gain. This is because of the solar panel and the air gaps in between the glass and solar panel fastened with plastic clasp (the circular disks in Fig. 22). The glass was only moderately fastened so that it does not to press the solar panel expressively, and not have the printed elements scratched off. The measured gain of the reflectarray

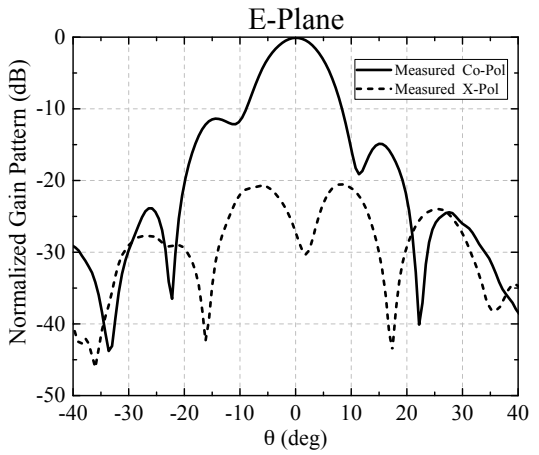


(a) E Plane Pattern.

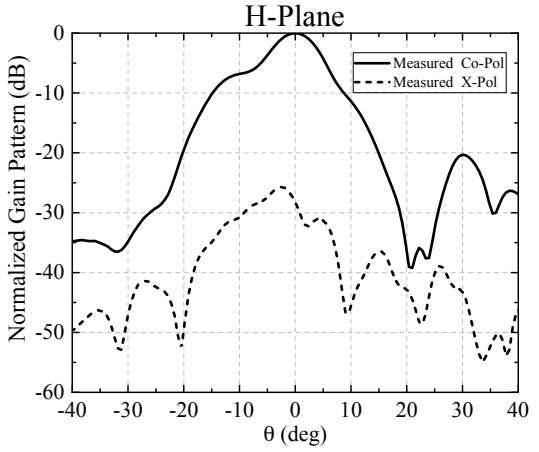


(b) H-Plane Pattern.

Fig. 17: Radiation Patterns of Inkjet Printed Reflectarray backed by a Metal Ground Plane without Solar Panel.



(a) Integration with Solar Panel E Plane Pattern.



(b) Integration with Solar Panel H-Plane Pattern.

Fig. 18: Radiation Patterns of Inkjet Printed Reflectarray on a Solar Panel backed by a Metal Ground Plane.

is listed in Table IV. As seen, when the array is fastened on a flat metal plate as tight as possible, the gain is very close to the simulation and the effect of printing (height and conductivity) is negligible, as analyzed in Section III-B. When there is some air (e.g. a thickness of 0.5 $\sim$ 1 mm), the gain reduces as discussed in Section III-C. It is roughly estimated that similar amount of air gap exists when the array is fastened onto the solar panel, based on the positions of the clasps' screws. Therefore, from Table IV, it is concluded that the gain reduction due to the solar panel is within 2 dB.

TABLE IV: Measured Gain and Aperture Efficiency

Antenna	Gain (dB)	η_{ap} (%)
No Air	24.35	45.2
Some Air	23.64	38.4
On Solar Panel	22.46	29.3

The measurements at WFF's spherical range in the anechoic chamber are summarized in Figs. 19, 20, where the antenna in Fig. 20 has been treated with Parylene HT. It is seen that the gain improved after the conformal coating. But it should be noted that the coating itself does not affect the gain to that extent. The coating is very thin and does not act as a lens to focus the beam. The reason for the gain improvement is that after the treatment, there was more comfort in handling the glass array and therefore it was fastened on the ground plane tighter than before, hence reducing the air gaps. It should also be noted that the incident bean angle was referenced as 0° at WFF and therefore the reflected beam is seen to be at $-22.7°$. So the measurements at USU are consistent with multiple tests at WFF.

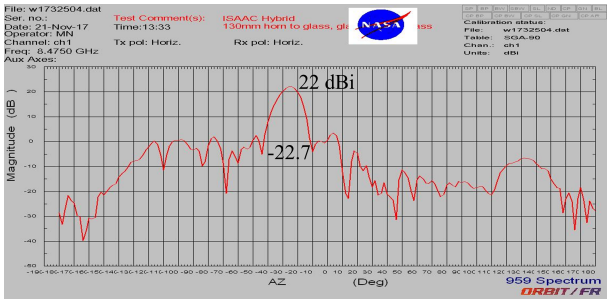


Fig. 19: Radiation Pattern Measured at WFF.

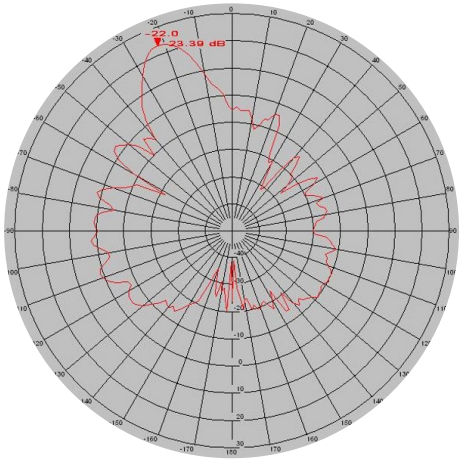


Fig. 20: Radiation Pattern Measured at WFF after Treating the Printed Glass with Protection Spray.

B. FINAL PROTOTYPE

A 20 cm $\times$ 30 cm solar panel was assembled at NASA Goddard Flight Center. SolAero ZTJM solar cells with 29% efficiency (now ZTJ series by Rocket Lab) were used [25]. Fig. 21 shows the final ISAAC prototype, and the Fig. 22 is ISAAC under test at the USU's near field-scanner. Measurement of ISAAC (Fig. 21) at WFF indicated a 17 dB gain, much lower than the design data. A close examination of the prototype revealed that an aluminum frame, as seen in Fig. 23 was used to elevate the glass from the solar panel. The frame is thicker than 2 mm. Therefore, this is consistent with the analysis in Section III-C. After the frame was carefully removed, the gain rose back to the 21-22 dB range as measured before the full assembly. It is therefore concluded that ISAAC met the design goal, and the future prototype for flight may consider a thinner spacer, as well as taking the spacer and air gap into the unit cell analysis.

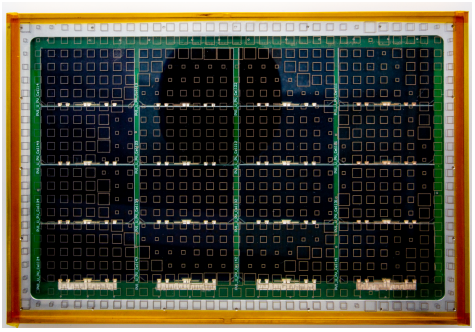


Fig. 21: ISAAC Prototype.

C. SOLAR PANEL PERFORMANCE

The solar panel's performance were assessed by measuring the current-voltage (I-V) and power-voltage (P-V) curves. The measurements at USU was performed by placing a half of the reflectarray on a 3U solar panel (SP) (Fig. 24) and the set-up is as described in [26]. The measurements at WFF were

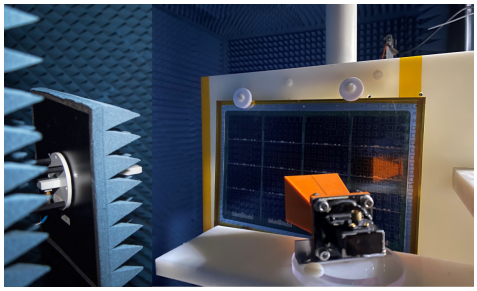


Fig. 22: ISAAC Test at USU.

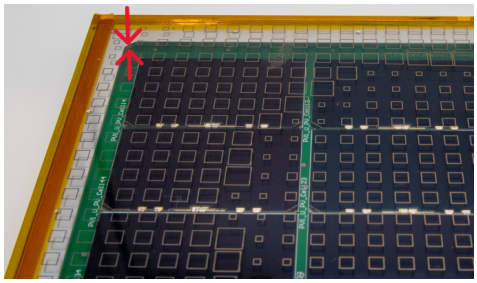


Fig. 23: Separation Frame.

performed on the final ISAAC. The results are presented in Figs. 25, 26. Fig. 25 shows that the power drop due to the reflectarray is $8.32 - 7.51 = 0.81$ W, indicating a degradation of 9.7% of power. But, it is deemed that a 10% degradation in power efficiency can be acceptable for power-positive missions. The SP efficiency can be calculated from the measured power as follows. Assuming that the bare cells function at 29%, as the plain glass has a transmittance of 92%, the incident power of the light source is $8.32/(0.29 \times 0.92) = 31.2$ W, and therefore the SP efficiency under the glass with printed reflectarray is $7.51 \div 31.2 = 24\%$, which is deemed acceptable for CubeSat missions. As a comparison, the SP efficiency under the plain glass is 26.7%.

The measurements from the USU's set-up includes a comparison of power on bare cells, with a plain AF32 glass, and under the printed glass. The solar panel efficiencies were calculated by measuring the incident power from the artificial light source illuminating the panel [26]. The results are summarized in Table V. It is clear that the plain AF32 glass reduces the efficiency for at least 2% and then the overall efficiency drop due to ISAAC is due to the combination of the glass the printed array. As seen, the measurements at USU and WFF are in agreement.

TABLE V: Solar Panel Efficiency Measured at USU

Test Set-up	SP Efficiency (%)
Bare SP	26.1
SP under clear AF32 Glass	24
SP under half-ISAAC on AF32	20.8

V. CONCLUSION

An optically transparent reflectarray antenna, ISAAC, with transparency and aperture efficiency higher than previous

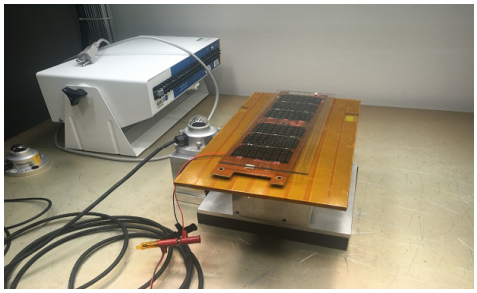
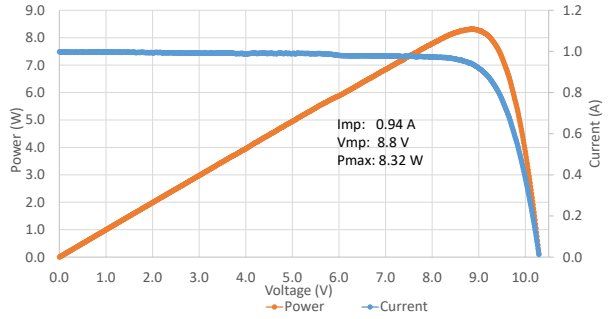
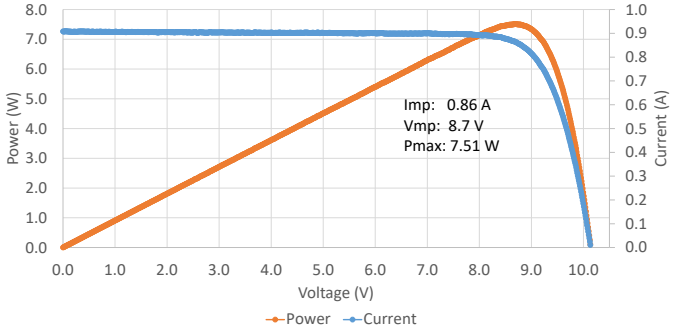


Fig. 24: Solar Panel Measurement Set-up at USU.



(a) IV Curve of the Solar Panel Covered with a Plain 2.5 mm AF32 Glass.

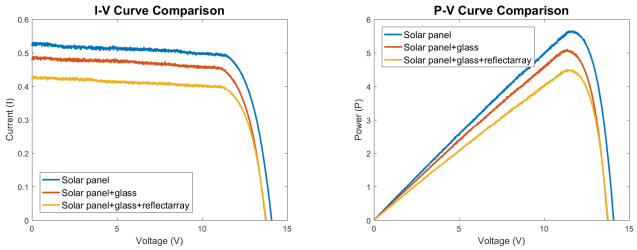


(b) IV Curve of ISAAC.

Fig. 25: IV Curve Measurement at Wallops.

publications is presented. Detailed examination on different unit cells were performed to select the most optimal geometry that produces the best optical transparency and antenna gain. The unit cells were examined for both half wavelength and sub-wavelength spacing. It is shown that a sub-wavelength design helps to manege the loss due to the radiating elements' finite conductivity and the semi-conductor solar cells. Loss due to assembly is also studied and method to analyze and estimate all these loss factors are presented. The reflectarray is prototyped using inkjet printing with conductive ink, which is a material efficient and very fast method.

The final design was fabricated and assembled using all COTS parts suitable for CubeSat deployment. The antenna operates at 8.475 GHz, and has a gain of higher than 21 dB after a full integration with the solar panel. The optical transparency of the antenna is 95%, and with the 92% transparent cover glass, ISAAC reduces the efficiency of a triple junction solar panel from 29% (bare cell) to 24%. The net reduction



(a) IV Curve. (b) PV Curve.

Fig. 26: Solar Panel Measurements at USU.

in power is less than 10% and is deemed acceptable for a 6U or larger CubeSat mission.

The size of ISAAC fits one face of a 6U CubeSat or a 3U Cubesat with a deployed panel. The achieved gain and transparency of ISAAC are higher than similar antennas reported when scaled to the same size. ISAAC resolves problems of competition between solar cells and high gain antenna when the light source and communication line of sight are along the same direction. The ISAAC frequency can be supported by both NEN and DSN and therefore suitable for a LEO CubeSat integration or relaying from Lunar orbit. The design can be easily extended to Ka band to relay upward from LEO to high orbit constellations such as Tracking and Data Relay Satellite (TDRS) or its successors. ISAAC design for now offers linear polarizations (TE or TM), but the design method can be easily extended to circular polarization.

An important learning experience from ISAAC is the assessment of the effect of solar cells. It is known that the solar cells are lossy and will reduce the antenna's gain. Studies on ISAAC design show that since the cover glass is much thicker than solar cells, the gain reduction due to the phase error caused by the thickness of solar cells is neglectable. The loss due to solar cells is also manageable because the thick cover glass supports effectively high reflection from unit cells. In addition, a sub-wavelength design contributes to loss reduction. When scaling up the frequency, however, such as redesigning ISAAC to Ka band, the thickness of solar cells may be comparable to the cover glass. In that case, it is important to include at least the thickness and dielectric constant of the solar cells into the unit cell design. A full wave simulation by incorporating a full solar cell model is certainly helpful if supported by computing power.

It is also found that a close communication between the solar panel assembly and the reflectarray design is critical. As ISAAC is printed on a single piece of glass, in order to leave room for the connections of solar cells and possible heat dissipation, the glass may need to be lifted up for a short distance from the solar panel. This distance should be discussed before the antenna design so that it can be included into the unit cell study to reduce phase error occurring from the solar panel integration.

REFERENCES

[1] Y. Rahmat-Samii, "Special issue on antenna innovations for cubesats and smallsats," *IEEE Antennas and Propagation Magazine*, pp. 16– 127, 2017.

[2] R. E. Hodges, M. J. Radway, A. Toorian, D. J. Hoppe, B. Shah, and A. E. Kalman, "Isara - integrated solar array and reflectarray cubesat deployable ka-band antenna," in *2015 IEEE International Symposium on Antennas and Propagation & USNC/URSI National Radio Science Meeting*, 2015, pp. 2141–2142.

[3] R. E. Hodges, N. Chahat, D. J. Hoppe, and J. D. Vacchione, "A deployable high-gain antenna bound for mars: Developing a new folded-panel reflectarray for the first cubesat mission to mars," *IEEE Antennas and Propagation Magazine*, vol. 59, no. 2, pp. 39–49, 2017.

[4] "Sport spacecraft (scintillation prediction observations research task)," 2024, accessed: 2026-03-25. [Online]. Available: https://www.nanosats.eu/sat/sports

[5] M. Zawadzki and J. Huang, "Integrated rf antenna and solar array for spacecraft application," in *Proceedings 2000 IEEE International Conference on Phased Array Systems and Technology (Cat. No.00TH8510)*, 2000, pp. 239–242.

[6] W. An, S. Xu, F. Yang, and J. Gao, "A ka-band reflectarray antenna integrated with solar cells," *IEEE Transactions on Antennas and Propagation*, vol. 62, no. 11, pp. 5539–5546, 2014.

[7] L. Xiong, W. An, C. Deng, H. Sun, S. Xu, and F. Yang, "A ka-band dual-band reflectarray antenna with solar cells," *IEEE Antennas and Wireless Propagation Letters*, vol. 23, no. 6, pp. 1889–1893, 2024.

[8] P. Dreyer, M. Morales-Masis, S. Nicolay, C. Ballif, and J. Perruisseau-Carrier, "Copper and transparent-conductor reflectarray elements on thin-film solar cell panels," *IEEE Transactions on Antennas and Propagation*, vol. 62, no. 7, pp. 3813–3818, 2014.

[9] M. A. Moharram and A. A. Kishk, "Optically transparent reflectarray antenna design integrated with solar cells," *IEEE Transactions on Antennas and Propagation*, vol. 64, no. 5, pp. 1700–1712, 2016.

[10] J. Oh, K. Lee, T. Hughes, S. Forrest, and K. Sarabandi, "Flexible antenna integrated with an epitaxial lift-off solar cell array for flapping-wing robots," *IEEE Transactions on Antennas and Propagation*, vol. 62, no. 8, pp. 4356–4361, 2014.

[11] H. Wang, Y. B. Park, and I. Park, "Low-profile wideband solar-cell-integrated circularly polarized cubesat antenna for the internet of space things," *IEEE Access*, vol. 10, pp. 61 451–61 462, 2022.

[12] O. O'Conchubhair, P. McEvoy, and M. J. Ammann, "Integration of antenna array with multicrystalline silicon solar cell," *IEEE Antennas and Wireless Propagation Letters*, vol. 14, pp. 1231–1234, 2015.

[13] W. An, H. Wang, J. Wang, Y. Luo, K. Ma, and J. Ma, "Low-profile wideband microstrip antenna integrated with solar cells," *IEEE Transactions on Antennas and Propagation*, vol. 70, no. 9, pp. 8530–8535, 2022.

[14] "Cubesat design specification rev. 13," available at https://www.cubesat.org/resources.

[15] National Aeronautics and Space Administration, "Cubesat 101: Basic concepts and processes for first-time cubesat developers," NASA CubeSat Launch Initiative, Tech. Rep., 2017, revision dated October 2017.

[16] T. Yekan, R. Baktur, and C. Swenson, "Examination of two types of quasi transparent reflectarray elements," in *2016 IEEE International Symposium on Antennas and Propagation (APSURSI)*, 2016, pp. 1543–1544.

[17] T. Yekan and R. Baktur, "A study of meshed patch reflectarray unit cell," in *2016 IEEE International Symposium on Antennas and Propagation (APSURSI)*, 2016, pp. 1711–1712.

[18] ——, "Design of two transparent x band reflectarray antennas integrated on a satellite panel," in *2016 IEEE International Symposium on Antennas and Propagation (APSURSI)*, 2016, pp. 1413–1414.

[19] T. Yekan, R. Baktur, C. Swenson, O. Kegege, S. Altunc, H. Shaw, J. Lyons, and M. Deshpande, "Transparent reflectarray antenna printed on solar cells," in *2016 IEEE 43rd Photovoltaic Specialists Conference (PVSC)*, 2016, pp. 2610–2612.

[20] D. Pozar, S. Targonski, and H. Syrigos, "Design of millimeter wave microstrip reflectarrays," *IEEE Transactions on Antennas and Propagation*, vol. 45, no. 2, pp. 287–296, 1997.

[21] R. Baktur, "Cubesat link budget: Elements, calculations, and examples," *IEEE Antennas and Propagation Magazine*, vol. 64, no. 6, pp. 16–28, 2022.

[22] N. G. R. Center, "Game changing development program: Solar power generation in extreme space environments," NASA Technical Reports Server (NTRS), Cleveland, OH, 2016, fS-2016-07-048-GRC, PS-01986–0816. [Online]. Available: https://ntrs.nasa.gov/api/citations/20170004553/downloads/20170004553.pdf

[23] The SCHOTT Group, https://www.schott.com/en-us, accessed: 2026-03-31.

[24] K. K. Karnati, Y. Yusuf, S. Ebadi, and X. Gong, "Theoretical analysis on reflection properties of reflectarray unit cells using quality factors," *IEEE Transactions on Antennas and Propagation*, vol. 61, no. 1, pp. 201–210, 2013.

[25] Rocket Lab, "Space solar cells - cics," Rocket Lab, 2023, accessed: 2023-04-27. [Online]. Available: https://rocketlabcorp.com/space-systems/solar/space-solar-cellscics/

[26] T. Yekan and R. Baktur, "An x band patch antenna integrated with commercial triple-junction space solar cells," *Microwave and Optical Technology Letters*, vol. 59, no. 2, pp. 260–265, 2017. [Online]. Available: https://onlinelibrary.wiley.com/doi/abs/10.1002/mop.30275

[27] ——, "An experimental study on the effect of commercial triple junction solar cells on patch antennas integrated on their cover glass," *Progress In Electromagnetics Research C*, vol. 63, pp. 131–142, 2016.

[28] ——, "Study of the impact between a triple junction space solar cell and the antenna integrated on top of it," *IEEE Transactions on Antennas and Propagation*, vol. 69, no. 3, pp. 1734–1739, 2021.

[29] T. W. Turpin and R. Baktur, "Meshed patch antennas integrated on solar cells," *IEEE Antennas and Wireless Propagation Letters*, vol. 8, pp. 693–696, 2009.

[30] T. Day and R. Baktur, "Optically transparent solar panel integrated patch antenna for small satellite applications," in *2025 IEEE International Symposium on Antennas and Propagation and North American Radio Science Meeting (AP-S/CNC-USNC-URSI)*, 2025, pp. 1025–1027.

[31] J. Shaker, M. Chaharmir, and J. Ethier, *Reflectarray Antennas: Analysis, Design, Fabrication and Measurement*. Artech House, 2013.

[32] J. Ethier, M. R. Chaharmir, and J. Shaker, "Loss reduction in reflectarray designs using sub-wavelength coupled-resonant elements," *IEEE Transactions on Antennas and Propagation*, vol. 60, no. 11, pp. 5456–5459, 2012.

[33] D. Pozar, "Wideband reflectarrays using artificial impedance surfaces," *Electronics letters*, vol. 43, no. 3, pp. 148–149, 2007.

[34] A. Yu, F. Yang, A. Z. Elsherbeni, J. Huang, and Y. Rahmat-Samii, "Aperture efficiency analysis of reflectarray antennas," *Microwave and Optical Technology Letters*, vol. 52, no. 2, pp. 364–372, 2010.

[35] Novacentrix, https://novacentrix.com/, Novacentrix, Inc., 2026, accessed: 2026-04-29.

[36] FUJIFILM Dimatix Materials Printer, https://www.fujifilm.com/us/en/business/inkjet-solutions/inkjet-technology-integration/dmp-2850, accessed: 2026-04-29.

[37] O. Azucena, J. Kubby, D. Scarbrough, and C. Goldsmith, "Inkjet printing of passive microwave circuitry," in *2008 IEEE MTT-S International Microwave Symposium Digest*, 2008, pp. 1075–1078.



Taha Yekan received his B.Sc. degree from Iran University of Science and Technology in 2008, his M.Sc. degree from Sharif University of Technology in 2010, and his Ph.D. degree from Utah State University in 2016. He is an antenna and system engineer. His research interests include antenna design, RF and microwave systems, phased-array antennas, 5G technologies, and wireless communication systems..



Muhammadeziz Tuyghur received his M.Sc. degree from Utah State University in 2017, and the Ph.D. degree in electrical and computer engineering from University of Wisconsin-Madison, Madison, WI, USA, in 2022. His research interests include electromagnetics, antenna design, printed antennas and RF front-end module development for next-generation wireless communication systems.



Serhat Altunc Serhat Altunc received his PhD in Electrical Engineering from University of New Mexico in 2007. He is currently working at Goddard Space flight Center, NASA on multiple Satellite and Ground Communication Research activities . He is a flight and ground communication technologist with antenna, RF and Communication systems background. He published over 100 papers in refereed journals, book chapter, conference proceedings and presentations.



Eleanya E. Onuma holds a B.S. in Applied Mathematics from Bowie State University, a B.S. in Electrical Engineering from Morgan State University, and an M.S. in Electrical Engineering from the Johns Hopkins University (Whiting School of Engineering). He has over 15 years of aerospace experience designing, developing, integrating, testing, and operating fiber-based photonics assemblies.



Marta Shelton is an AeroSpace Engineer and a 10-year NASA veteran. She attended Purdue University with a Master's Degree from VA Tech. Marta is a Communications subject matter expert and antenna designer, and had been the lead engineer of a NASA Anechoic Test Chamber. She is an advocate of cutting-edge technologies such as the clear antenna and lately optical communications. Marta held titles such as Assistant Director of Engineering. In 2026 , Marta is the technical lead for NASA's Space Communications and Navigation, Commercialization, Innovation and Synergies office.



REYHAN BAKTUR (Senior Member, IEEE) received the Ph.D. degree in electrical and computer engineering from Clemson University, Clemson, South Carolina, in 2005. She joined the department of electrical and computer engineering at Utah State University, Logan, Utah in 2006, and is currently an associate professor. Dr. Baktur is an IEEE Distinguished Lecturer of 2022–2024. Her research interests include antenna design for CubeSats, optically transparent antennas, and integrated solar panel antennas.